

**IMMOBILIZED TiO₂/ACTIVATED CARBON BILAYER SYSTEM FOR THE
REMOVAL OF PHENOL VIA PHOTOCATALYTIC-ADSORPTIVE
PROCESSES**

NOOR NAZIHAH BINTI BAHRUDIN

UNIVERSITI SAINS MALAYSIA

2012

**IMMOBILIZED TiO₂/ACTIVATED CARBON BILAYER SYSTEM FOR THE
REMOVAL OF PHENOL VIA PHOTOCATALYTIC-ADSORPTIVE
PROCESSES**

by

NOOR NAZIHAH BINTI BHRUDIN

**Thesis submitted in fulfillment of the requirements
for the degree of
Master of Science**

APRIL 2012

AKNOWLEDGEMENTS

IN THE NAME OF ALLAH THE MOST GRACIOUS AND MOST MERCIFUL

Alhamdulillah. All praises to Allah S.W.T for blessing me with health, courage and ease to complete this research and thesis successfully. Heartfelt thanks to my supervisor, Professor Dr Hj Mohd Asri Nawawi who had given this amazing opportunity to be guided and supervised by him. His supportive advice, patience, guidance, motivation and inspiration along the way are those money can't buy.

I would also like to acknowledge the following organizations for the financial aid and grant-funding: Ministry of Higher Education (MOHE) under Bajet Mini Programme (2009-2010) and Universiti Sains Malaysia (USM) for Graduate Assistant Scheme (2009-2011), Postgraduate Research Grant (PGRS:1001/PKIMIA/843034) and research facilities provided. Not to be forgotten, my sincere thanks to all the staffs from School of Chemical Sciences, School of Biological Sciences, School of Physical Sciences, School of Chemical Engineering and Institute of Postgraduate Studies (IPS) for the cooperation and assistance ship.

My endless appreciation then goes to the most important people in my life, my parents, Hj Bahrudin Daud, Hj Maimunah Yunus and my two sisters, Maisarah and Yuhani for their continuous moral and financial support during the hard moments I had in completing the studies. Thank you for believing in me. Special thanks are also forwarded to Mrs Salmiah Md Zain for the data sharing, all graduate students in Photocatalysis Laboratory and my close friends for their generous encouragement. Last but not least, I would like to share my favorite quote, "Nobody can go back and start a new beginning, but anyone can start today and make a new ending." by Maria Robinson. Hopefully, this thesis would give everyone benefits.

TABLE OF CONTENTS

Acknowledgements	ii
Table of Contents	iii
List of Tables	xi
List of Figures	xiii
List of Plates	xix
List of Abbreviations	xxi
Abstrak	xxii
Abstract	xxiv

CHAPTER 1: INTRODUCTION AND LITERATURE REVIEWS

1.1	Water Pollution: Law Enforcement, Treatment and Remediation Technology	1
1.2	Phenol	4
1.3	Environmental Photocatalysis	6
1.4	Titanium Dioxide as photocatalyst	8
1.5	Commercial TiO ₂	11
1.6	Photodegradation kinetic	14
1.7	Adsorption	15
1.8	Activated Carbon (AC)	16
1.9	Adsorption kinetic	21
1.9.1	Pseudo first order	21
1.9.2	Pseudo second order	22
1.9.3	Intraparticle diffusion	22
1.9.4	Elovich model	23

1.10	Combination of photocatalysis and adsorption processes as a single system.	23
1.11	The equilibrium adsorption isotherm models	24
1.12	Various methods of coupling TiO ₂ and AC in the removal of pollutants.	28
1.13	Immobilization of TiO ₂ /AC in the form of a bilayer system	31
1.14	Polymer blend as adhesives	33
	1.14.1 Epoxidized Natural Rubber (ENR)	34
	1.14.2 Polivinyll Chloride (PVC)	35
1.15	Problem Statements	36
1.16	Research objectives	37
CHAPTER 2: METHODOLOGY		
2.1	Chemicals and reagents	39
2.2	Instruments and Equipments	39
2.3	Treatment of Activated Carbon	41
2.4	Determination of properties of activated carbon	41
	2.4.1 Iodine number	42
	2.4.2 Ash content	43
	2.4.3 pH	44
	2.4.4 Determination of point of zero charge (pH _{pzc}) of powdered activated carbon	44
2.5	Preparation of 10 mg L ⁻¹ phenol solution	44
2.6	Preparation of eluent (mobile phase)	45
2.7	Preparation of Epoxidized Natural Rubber (ENR ₅₀)	45
	2.7.1 Determination of Toluene to ENR ₅₀ concentration in toluene.	46
2.8	Preparation of high range COD reagent for COD analysis	46

2.9	Preparation of ENR ₅₀ /PVC polymer blend	47
2.10	Preparation of TiO ₂ /ENR ₅₀ /PVC dip-coating solution	48
2.11	Preparation of AC/ENR ₅₀ /PVC dip-coating solution	48
2.12	Fabrication of immobilized TiO ₂ /ENR ₅₀ /PVC, AC/ENR ₅₀ /PVC and TiO ₂ /AC/ENR ₅₀ /PVC on the glass plates	49
2.13	Batch reactor setup	49
	2.13.1 Photocatalysis studies using immobilized mode system	51
	2.13.2 Photocatalytic studies using the TiO ₂ slurry mode system	51
	2.13.3 Adsorption studies using immobilized and TiO ₂ slurry mode systems	52
2.14	Analysis of phenol	52
2.15	Photocatalytic degradation of phenol by immobilized TiO ₂ /ENR ₅₀ /PVC	53
	2.15.1 Effect of the TiO ₂ /ENR ₅₀ /PVC loading on the photocatalytic activity of the immobilized system	53
2.16	Preparation of AC/ENR/PVC dip-coating solution	54
	2.16.1 Optimization of ENR ₅₀ in AC/ENR ₅₀ /PVC dip-coating solution.	54
	2.16.2 Optimization of PVC in AC/ENR ₅₀ /PVC dip-coating solution	55
2.17	Adherence test of the immobilized AC/ENR ₅₀ /PVC plates	55
2.18	Characterization of TiO ₂ /ENR ₅₀ /PVC, AC/ENR ₅₀ /PVC and TiO ₂ /AC/ENR ₅₀ /PVC	56
	2.18.1 Scanning Electron Microscopy (SEM)	56
	2.18.2 Energy Dispersive X-Ray (EDX)	57
	2.18.3 Fourier-Transform Infra Red (FT-IR) analysis	57
	2.18.4 Thermogravimetric (TGA) analysis	57
	2.18.5 Brunauer, Emmett and Teller (BET) analysis	58

2.14.6	CHN analysis	58
2.14.7	Photoluminescence (PL) spectroscopic analysis	59
2.19	Adsorption of phenol study by immobilized AC/ENR ₅₀ /PVC and TiO ₂ /AC/ENR ₅₀ /PVC.	59
2.19.1	Effect of AC/ENR ₅₀ /PVC loading on adsorption of phenol	59
2.19.2	Effect of initial pH on adsorption of phenol by immobilized AC/ENR ₅₀ /PVC.	59
2.19.3	Effect of initial phenol concentration and contact time	60
2.20	Photocatalytic degradation of phenol by TiO ₂ /AC/ENR ₅₀ /PVC bilayer system.	60
2.20.1	Effect of TiO ₂ /ENR ₅₀ /PVC loading on photocatalytic activity of TiO ₂ /AC/ENR ₅₀ /PVC.	60
2.20.2	Effect of AC/ENR ₅₀ /PVC loading on photocatalytic activity of TiO ₂ /AC/ENR ₅₀ /PVC bilayer system.	61
2.20.3	Effect of initial pH solution on the photocatalytic-adsorption removal of phenol by TiO ₂ /AC/ENR ₅₀ /PVC bilayer system.	62
2.20.4	Effect of dissolved oxygen on photocatalytic-adsorption removal of phenol by TiO ₂ /AC/ENR ₅₀ /PVC bilayer system.	62
2.20.5	Effect of initial phenol concentration on the photocatalytic – adsorption removal of phenol by the TiO ₂ /AC/ENR ₅₀ /PVC bilayer system.	63
2.20.6	Effect of UV irradiance light intensity on the photocatalytic degradation of phenol by TiO ₂ /AC/ENR ₅₀ /PVC bilayer system.	63
2.21	Reusability study of the fabricated TiO ₂ /AC/ENR ₅₀ /PVC and TiO ₂ /ENR ₅₀ /PVC plates on the removal of phenol under fluorescent lamp and solar irradiation.	64
2.22	The degradation of organic polymers in the immobilized TiO ₂ /AC/ENR ₅₀ /PVC, TiO ₂ /ENR ₅₀ /PVC and AC/ENR ₅₀ /PVC systems.	64
2.22.1	COD analysis	65
2.23	Mineralization study of phenol solutions	65

2.23.1	COD analysis	65
--------	--------------	----

CHAPTER 3: RESULTS AND DISCUSSIONS

3.1	Evaluation on photoactivity and adsorption of the system	67
3.2	TiO ₂ /ENR ₅₀ /PVC dip-coating solution	68
3.3	Immobilized TiO ₂ /ENR ₅₀ /PVC single layer study	71
3.3.1	Photocatalytic degradation of phenol	71
3.3.2	Effect of TiO ₂ /ENR ₅₀ /PVC loading on the photocatalytic activity of the immobilized system	73
3.4	Determination of properties of activated carbon	77
3.5	Fabrication of TiO ₂ /ENR ₅₀ /PVC, AC/ENR ₅₀ /PVC and TiO ₂ /AC/ENR ₅₀ /PVC on the glass plates	78
3.6	AC/ENR ₅₀ /PVC dip-coating solution	80
3.6.1	Optimization of ENR ₅₀ in AC/ENR ₅₀ /PVC dip-coating solution	80
3.6.2	Coating adherence	84
3.6.3	Optimization of PVC in AC/ENR ₅₀ /PVC dip-coating solution	86
3.6.4	Coating adherence	89
3.7	Characterizations of AC/ENR ₅₀ /PVC composite	91
3.7.1	SEM-EDX analysis	91
3.7.2	BET analysis	94
3.7.3	CHN analysis	95
3.7.4	FT-IR analysis	96
3.8	Adsorption of phenol by immobilized AC/ENR ₅₀ /PVC and TiO ₂ /AC/ENR ₅₀ /PVC	98
3.8.1	Effect of AC/ENR ₅₀ /PVC loading on the adsorption of phenol	98

3.8.2	Effect of initial pH on adsorption of phenol by immobilized AC/ENR ₅₀ /PVC	101
3.8.3	Effect of initial concentrations and contact time	103
3.8.4	Adsorption kinetics study	109
3.8.5	Adsorption isotherm study	113
3.9	TiO ₂ /AC/ENR ₅₀ /PVC bilayer system for the removal of phenol from aqueous solution.	116
3.9.1	Control test	116
3.9.2	PL analysis	118
3.10	Photocatalytic degradation of phenol by TiO ₂ /AC/ENR ₅₀ /PVC bilayer system.	120
3.10.1	Effect of TiO ₂ /ENR ₅₀ /PVC loading on the photocatalytic activity of TiO ₂ /AC/ENR ₅₀ /PVC.	120
3.10.2	Effect of AC/ENR ₅₀ /PVC loading on the photocatalytic activity of TiO ₂ /AC/ENR ₅₀ /PVC bilayer system.	130
3.10.3	Effect of initial pH solution on the photocatalytic- adsorption removal of phenol by TiO ₂ /AC/ENR ₅₀ /PVC bilayer system.	137
3.10.4	Effect of dissolved oxygen on the photocatalytic-adsorption removal of phenol by TiO ₂ /AC/ENR ₅₀ /PVC bilayer system.	141
3.10.5	Effect of initial concentrations on the photocatalytic–adsorption removal of phenol by the TiO ₂ /AC/ENR ₅₀ /PVC bilayer system.	144
3.10.6	Effect of UV irradiance light intensity on the photocatalytic degradation of phenol by TiO ₂ /AC/ENR ₅₀ /PVC bilayer system.	147
3.11	Comparison of removal efficiency of phenol by TiO ₂ /ENR ₅₀ /PVC and TiO ₂ /AC/ENR ₅₀ /PVC systems.	149
3.12	Application of TiO ₂ /AC/ENR ₅₀ /PVC and TiO ₂ /ENR ₅₀ /PVC single layer systems under solar irradiation.	157
3.13	Reusability of the TiO ₂ /AC/ENR ₅₀ /PVC bilayer system	159
3.14	Monitoring the degradation of polymeric binders into the system	166
3.14.1	COD test	168

3.14.2	TGA analysis	170
3.15	Comparison of mineralization of phenol by TiO ₂ /AC/ENR ₅₀ /PVC and TiO ₂ /ENR ₅₀ /PVC.	174
3.16	Comparison of TiO ₂ /ENR ₅₀ /PVC and AC/ENR ₅₀ /PVC layers before and after applications.	179
3.16.1	SEM-EDX analysis	179
3.16.2	CHN analysis	185
3.16.3	FT-IR analysis	186
CHAPTER 4: CONCLUSIONS		188
4.1	Conclusions	188
4.2	Future works	191
REFERENCES		193
APPENDICES		
Appendix A	Calculation	206
Appendix B	Additional graphs	207
Appendix C	Additional tables	212
Appendix D	List of publications and seminars	213

LIST OF TABLE

Table 1.1	Characteristics of ideal and green chemistry	2
Table 1.2	Available technologies for use in the wastewater treatment	3
Table 1.3	Commercial TiO ₂ s and their properties	12
Table 1.4	Type of ACs and their properties.	17
Table 1.5	Classification of AC pores.	18
Table 1.6	Models of isotherm.	26
Table 2.1	Physical properties and their respective analyses	42
Table 3.1	BET results for different immobilized TiO ₂ /ENR ₅₀ /PVC loadings.	76
Table 3.2	Physical properties of AC powder before and after acid treatment.	78
Table 3.3	BET surface area of AC before and after the addition of ENR ₅₀ and PVC	95
Table 3.4	CHN analysis of AC powder before and after the addition of ENR ₅₀ and PVC	96
Table 3.5	BET result for different loadings of immobilized AC/ENR ₅₀ /PVC.	100
Table 3.6	Point of zero charge of AC powder and AC/ENR ₅₀ /PVC dip-coating solution.	103
Table 3.7	Kinetic parameters for the adsorption of phenol into immobilized AC/ENR ₅₀ /PVC single layer system.	112
Table 3.8	Kinetic parameters for the adsorption of phenol into TiO ₂ /AC/ENR ₅₀ /PVC bilayer system	112
Table 3.9	Langmuir isotherm constants and correlation coefficient for phenol adsorption at different concentrations.	114
Table 3.10	Freundlich isotherm constants and correlation coefficients for phenol adsorption at different concentrations.	114
Table 3.11	Separation factors, R _L and type of isotherms	115
Table 3.12	R _L values for adsorption of phenol onto AC/ENR ₅₀ /PVC and	115

TiO₂/AC/ENR₅₀/PVC at different initial concentrations.

Table 3.13	Cross section thickness of immobilized TiO ₂ /ENR ₅₀ /PVC at fixed AC/ENR ₅₀ /PVC loadings.	130
Table 3.14	Cross section thickness of immobilized AC/ENR ₅₀ /PVC at fixed TiO ₂ /ENR ₅₀ /PVC loading.	137
Table 3.15	Point of zero charge of TiO ₂ P-25 powder and TiO ₂ /ENR ₅₀ /PVC dip-coating solution.	140
Table 3.16	EDX analysis of TiO ₂ /ENR ₅₀ /PVC and AC/ENR ₅₀ /PVC layer before and after applications	185
Table 3.17	CHN analysis of TiO ₂ /ENR ₅₀ /PVC and AC/ENR ₅₀ /PVC layers before and after applications	186

LIST OF FIGURES

Figure 1.1	Molecular structure of phenol.	4
Figure 1.2	Schematic diagram of TiO ₂ photocatalysis mechanism.	10
Figure 1.3	Number of publications on commercial TiO ₂ .	13
Figure 1.4	Schematic diagram of relationships between the three components of the adsorption system.	16
Figure 1.5	Basic flow sheet for activation of activated carbon.	20
Figure 1.6	Illustration of photocatalyst and adsorbent coated on a supporting material to form a TiO ₂ -AC bilayer system.	33
Figure 2.1	Indoor photocatalytic reactor set-up.	50
Figure 2.2	Solar photocatalytic reactor set-up.	50
Figure 3.1	Pseudo first order rate constant and percentage removal of phenol on photocatalytic degradation and adsorption using TiO ₂ suspension and photolysis. Experimental conditions: TiO ₂ : 0.32 mg cm ⁻² or 0.5 g L ⁻¹ for suspension, aeration flow rate: 100 mL min ⁻¹ , pH solution: 6.3, initial phenol concentration: 10 mg L ⁻¹ , light intensity: 6.0 W m ⁻² of 45W fluorescent lamp.	72
Figure 3.2	Pseudo first order rate constant of three consecutive runs on the effect of different TiO ₂ /ENR ₅₀ /PVC loadings on photocatalytic degradation of phenol. Experimental conditions: Aeration flow rate: 100 mL min ⁻¹ , pH solution: 6.3, initial phenol concentration: 10 mg L ⁻¹ , light intensity: 6.0 W m ⁻² of 45W fluorescent lamp.	75
Figure 3.3	The effect of the different amount of ENR ₅₀ at fixed amount of 0.8 g PVC powder in AC/EN ₅₀ /PVC dip-coating solution on the pseudo second order rate constants for three runs on the removal of phenol by degradation using TiO ₂ /AC/ENR ₅₀ /PVC via photocatalytic-adsorption processes. Experimental conditions: TiO ₂ /AC loadings: 0.32 mg cm ⁻² /0.32 mg cm ⁻² , aeration flow rate: 100 mL min ⁻¹ , initial phenol concentration: 10 mg L ⁻¹ , light intensity: 6.0 W m ⁻² of 45W fluorescent lamp.	82
Figure 3.4	The effect of different amount of ENR ₅₀ at fixed amount of 0.8 g PVC powder in AC/ENR ₅₀ /PVC dip-coating solution on the percentage of removal of phenol by the immobilized via photocatalytic-adsorption processes by TiO ₂ /AC/ENR ₅₀ /PVC system for 90 minutes of irradiation. Experimental conditions: TiO ₂ /AC loadings: 0.32 mg cm ⁻² /0.32 mg cm ⁻² , aeration flow rate: 100 mL min ⁻¹ , initial phenol concentration: 10 mg L ⁻¹ , light intensity: 6.0 W m ⁻² of 45W fluorescent lamp.	83

Figure 3.5	Percentage of the remaining AC/ENR ₅₀ /PVC layer on the glass plate after 15 s of sonication with the immobilized layer prepared using different amount of ENR ₅₀ at a fixed amount of 0.8 g PVC powder in the AC/ENR ₅₀ /PVC dip-coating solution.	85
Figure 3.6	The effect of different amount of PVC powder at fixed amount of 2 g ENR ₅₀ in AC/ENR ₅₀ /PVC formulation on the pseudo second order rate constants for the three consecutive runs on the removal of phenol via adsorption-photocatalysis processes by TiO ₂ /AC/ENR ₅₀ /PVC system for 90 minutes of irradiation. Experimental conditions: TiO ₂ /AC: 0.32 mg cm ⁻² /0.32 mg cm ⁻² , aeration flow rate: 100 mL min ⁻¹ , initial phenol concentration: 10 mg L ⁻¹ , light intensity: 6.0 W m ⁻² of 45W fluorescent lamp.	87
Figure 3.7	The effect of the different amount of PVC powder at fixed amount of 2 g ENR ₅₀ in AC/ENR ₅₀ /PVC dip-coating formulation on the percentage of removal phenol for three consecutive runs on via adsorption-photocatalysis processes by TiO ₂ /AC/ENR ₅₀ /PVC system for 90 minutes of irradiation. Experimental conditions: TiO ₂ /AC loadings: 0.32 mg cm ⁻² /0.32 mg cm ⁻² , aeration flow rate: 100 mL min ⁻¹ , initial phenol concentration: 10 mg L ⁻¹ , light intensity: 6.0 W m ⁻² of 45W fluorescent lamp.	88
Figure 3.8	Percentage of remaining AC/ENR ₅₀ /PVC on the glass plate after 15 s of sonication for plates prepared using dip-coating solution with different amount of PVC powder and at a fixed amount of 2 g ENR ₅₀ .	90
Figure 3.9	Combined FT-IR spectrum for AC powder before and after the addition of ENR ₅₀ and PVC powder in AC/ENR ₅₀ /PVC formulation.	97
Figure 3.10	The effect of AC/ENR ₅₀ /PVC loading on the adsorption capacity and percentage removal of phenol. Experimental conditions: Initial pH: 6.3, aeration flow rate: 100 mL min ⁻¹ , initial phenol concentration: 10 mg L ⁻¹ .	99
Figure 3.11	The effect of initial pH of phenol solution on the adsorption capacity of immobilized AC/ENR ₅₀ /PVC layer. Experimental conditions: AC: 2.54 mg cm ⁻² , aeration flow rate: 100 mL min ⁻¹ , initial phenol concentration: 10 mg L ⁻¹ .	102
Figure 3.12	The effect of initial concentration and contact time in the adsorption capacity of AC/ENR ₅₀ /PVC for the adsorption of phenol. Experimental conditions: AC: 2.54 mg cm ⁻² , aeration flow rate: 100 mL min ⁻¹ .	105
Figure 3.13	The effect of initial concentration and contact time on the adsorption capacity of TiO ₂ /AC/ENR ₅₀ /PVC in the adsorption	106

	of phenol. Experimental conditions: TiO ₂ /AC loadings: 0.32 mg cm ⁻² /2.54 mg cm ⁻² , aeration flow rate: 100 mL min ⁻¹ .	
Figure 3.14	The effect of TiO ₂ /ENR ₅₀ /PVC loadings on the adsorption capacity and percentage removal of phenol. Experimental conditions: Initial pH: 6.3, aeration flow rate: 100 mL min ⁻¹ , initial phenol concentration: 10 mg L ⁻¹ .	108
Figure 3.15	Rate constant and percentage of phenol removal on photocatalytic degradation and adsorption using TiO ₂ /AC/ENR ₅₀ /PVC, TiO ₂ /ENR ₅₀ /PVC and AC/ENR ₅₀ /PVC. Experimental conditions: TiO ₂ /AC: 0.32 mg cm ⁻² /2.54 mg cm ⁻² , aeration flow rate: 100 mL min ⁻¹ , initial phenol concentration: 10 mg L ⁻¹ , light intensity: 6.0 W m ⁻² of 45W fluorescent lamp.	117
Figure 3.16	Photoluminescence spectra of different immobilized systems.	119
Figure 3.17	Pseudo second order rate constant of three consecutive runs for the effect of different TiO ₂ /ENR ₅₀ /PVC loading on TiO ₂ /AC/ENR ₅₀ /PVC photocatalytic degradation. Experimental conditions: AC: 0.32 mg cm ⁻² , aeration flow rate: 100 mL min ⁻¹ , initial phenol concentration: 10 mg L ⁻¹ , light intensity: 6.0 W m ⁻² of 45W fluorescent lamp.	122
Figure 3.18	Percentage of remaining phenol for three runs due to the effect of different TiO ₂ /ENR ₅₀ /PVC loading on the TiO ₂ /AC/ENR ₅₀ /PVC photocatalytic degradation. Experimental conditions: AC: 0.32 mg cm ⁻² , aeration flow rate: 100 mL min ⁻¹ , initial phenol concentration: 10 mg L ⁻¹ , light intensity: 6.0 W m ⁻² of 45W fluorescent lamp.	123
Figure 3.19	Pseudo second order rate constant of three runs for the photocatalytic degradation of phenol due to the effect of different AC/ENR ₅₀ /PVC loading in the TiO ₂ /AC/ENR ₅₀ /PVC system. Experimental conditions: TiO ₂ /ENR ₅₀ /PVC: 0.32 mg cm ⁻² , aeration flow rate: 100 mL min ⁻¹ , initial phenol concentration: 10 mg L ⁻¹ , light intensity: 6.0 W m ⁻² of 45W fluorescent lamp.	132
Figure 3.20	Percentage removal of phenol for three runs due to the effect of different AC/ENR ₅₀ /PVC loading in the TiO ₂ /AC/ENR ₅₀ /PVC system. Experimental conditions: TiO ₂ /ENR ₅₀ /PVC: 0.32 mg cm ⁻² , aeration flow rate: 100 mL min ⁻¹ , initial phenol concentration: 10 mg L ⁻¹ , light intensity: 6.0 W m ⁻² of 45W fluorescent lamp.	133
Figure 3.21	Pseudo second order rate constants for the removal of phenol due to the effect of initial pH of phenol by the TiO ₂ /AC/ENR ₅₀ /PVC bilayer system. Experimental conditions:	139

TiO₂/AC: 0.32 mg cm⁻²/2.54 mg cm⁻², aeration flow rate: 100 mL min⁻¹, initial phenol concentration: 10 mg L⁻¹, light intensity: 6.0 W m⁻² of 45W fluorescent lamp.

Figure 3.22	Pseudo second order rate constants due to the effect of aeration flow rate during the removal of phenol by TiO ₂ /AC/ENR ₅₀ /PVC system. Experimental conditions: TiO ₂ /AC: 0.32 mg cm ⁻² /2.54 mg cm ⁻² , initial pH: 6.3, initial phenol concentration: 10 mg L ⁻¹ , light intensity: 6.0 W m ⁻² of 45W fluorescent lamp.	143
Figure 3.23	Pseudo second order rate constants for the removal of phenol due to the effect of initial concentrations of phenol by the TiO ₂ /AC/ENR ₅₀ /PVC system. Experimental conditions: TiO ₂ /AC: 0.32 mg cm ⁻² /2.54 mg cm ⁻² , initial pH: 6.3, aeration flow rate: 100 mL min ⁻¹ , light intensity: 6.0 W m ⁻² of 45W fluorescent lamp.	145
Figure 3.24	The effect of different intensity of UV irradiance leakage from 45 W fluorescent lamps on the pseudo second order rate constants for the removal of phenol by the TiO ₂ /AC/ENR ₅₀ /PVC bilayer system. Experimental conditions: TiO ₂ /AC: 0.32 mg cm ⁻² /2.54 mg cm ⁻² , initial pH: 6.3, aeration flow rate: 100 mL min ⁻¹ , initial concentration: 10 mg L ⁻¹ .	148
Figure 3.25	Comparison of the effect of initial pH of phenol on its percentage removal by TiO ₂ /AC/ENR ₅₀ /PVC bilayer and TiO ₂ /ENR ₅₀ /PVC single layer systems.	150
Figure 3.26	Comparison of percentage removal of phenol due to the the effect of aeration flow rates by the TiO ₂ /AC/ENR ₅₀ /PVC and TiO ₂ /ENR ₅₀ /PVC systems.	152
Figure 3.27	Comparison of percentage removal of phenol due to the effect of initial concentration of phenol solutions by the TiO ₂ /AC/ENR ₅₀ /PVC and TiO ₂ /ENR ₅₀ /PVC systems.	154
Figure 3.28	Comparison of percentage removal of phenol by the TiO ₂ /AC/ENR ₅₀ /PVC and TiO ₂ /ENR ₅₀ /PVC systems under the effect of the different intensity of UV irradiance leakage from the respective visible light fluorescent lamps.	156
Figure 3.29	Comparison on the percentage of removal of phenol by TiO ₂ /AC/ENR ₅₀ /PVC and TiO ₂ /ENR ₅₀ /PVC under solar and 45 W fluorescent lamp irradiation.	158
Figure 3.30	Reusability of TiO ₂ /AC/ENR ₅₀ /PVC and TiO ₂ /ENR ₅₀ /PVC plates for 10 consecutive runs in the removal of 10 mg L ⁻¹ phenol under irradiation of 45W fluorescent lamp.	161

Figure 3.31	Reusability of immobilized TiO ₂ /AC/ENR ₅₀ /PVC and TiO ₂ /ENR ₅₀ /PVC plates for 10 consecutive runs in the removal of 60 mg L ⁻¹ phenol under irradiation of 45W fluorescent lamp.	162
Figure 3.32	Reusability of TiO ₂ /AC/ENR ₅₀ /PVC and TiO ₂ /ENR ₅₀ /PVC plates for 10 consecutive runs in photocatalytic degradation of 10 mg L ⁻¹ phenol under solar irradiation.	164
Figure 3.33	Reusability of TiO ₂ /AC/ENR ₅₀ /PVC and TiO ₂ /ENR ₅₀ /PVC plates for 10 consecutive runs in photocatalytic degradation of 60 mg L ⁻¹ phenol under solar irradiation.	165
Figure 3.34	Reusability of TiO ₂ /AC/ENR ₅₀ /PVC and TiO ₂ /ENR ₅₀ /PVC plates for 10 consecutive runs in photocatalytic degradation of 60 mg L ⁻¹ phenol under solar irradiation.	169
Figure 3.35	Derivative thermogravimetric (DTG) curves of TiO ₂ /ENR ₅₀ /PVC dip-coating solution of 0, 1, 3 and 5 hours of irradiation	172
Figure 3.36	Derivative thermogravimetric (DTG) curves of AC/ENR ₅₀ /PVC dip-coating solution of 0, 1, 4 and 6 hours of irradiation.	173
Figure 3.37	COD values as a function of irradiation time in mineralization of 10 mg L ⁻¹ phenol by TiO ₂ /AC/ENR ₅₀ /PVC and TiO ₂ /ENR ₅₀ /PVC under fluorescent lamp. TiO ₂ /AC: 0.32 mg cm ⁻² /2.54 mg cm ⁻² , aeration flow rate: 100 mL min ⁻¹ , light source: 6.0 W m ⁻² of 45W fluorescent lamp.	175
Figure 3.38	COD values as a function of irradiation time in mineralization of 10 mg L ⁻¹ phenol by TiO ₂ /AC/ENR ₅₀ /PVC and TiO ₂ /ENR ₅₀ /PVC under solar irradiation. Experimental conditions: TiO ₂ /AC: 0.32 mg cm ⁻² /2.54 mg cm ⁻² , aeration flow rate: 100 mL min ⁻¹ , light source: solar.	177
Figure 3.39	COD values as a function of irradiation time in mineralization of 60 mg L ⁻¹ phenol by TiO ₂ /AC/ENR ₅₀ /PVC and TiO ₂ /ENR ₅₀ /PVC under solar irradiation. Experimental conditions: TiO ₂ /AC: 0.32 mg cm ⁻² /2.54 mg cm ⁻² , aeration flow rate: 100 mL min ⁻¹ , light source: solar.	178
Figure 3.40	FT-IR spectra of TiO ₂ /ENR ₅₀ /PVC layer before and after ten runs.	187
Figure 3.41	FT-IR spectra of AC/ENR ₅₀ /PVC layer before and after ten runs.	187

LIST OF PLATES

Plate 3.1	Surface morphology of TiO ₂ powder under 30 000 x magnification.	70
Plate 3.2	Surface morphology of TiO ₂ /ENR ₅₀ /PVC under 5 000 x magnification.	70
Plate 3.3	Surface morphology of TiO ₂ /ENR ₅₀ /PVC under 30 000 x magnification.	71
Plate 3.4	(a) Glass plate, (b) AC/ENR ₅₀ /PVC coated as the sub layer on the glass plate and (c) TiO ₂ /ENR ₅₀ /PVC coated on the AC/ENR ₅₀ /PVC layer as the upper layer on the same glass plate to produce TiO ₂ /AC/ENR ₅₀ /PVC/glass bilayer system.	79
Plate 3.5	Surface morphology of AC powder before acid treatment at 50 000 x magnification.	91
Plate 3.6	Surface morphology of AC powder after acid treatment at 50 000 x magnification.	92
Plate 3.7	Surface morphology of AC/ENR ₅₀ /PVC at 5 000 x magnification.	92
Plate 3.8	Surface morphology of AC/ENR ₅₀ /PVC at 50 000 x magnification.	93
Plate 3.9	Surface morphology of 0.32 mg cm ⁻² TiO ₂ /ENR ₅₀ /PVC loading at 1 000 x magnification.	125
Plate 3.10	Surface morphology of 0.32 mg cm ⁻² TiO ₂ /ENR ₅₀ /PVC loading at 50 000 x magnification.	125
Plate 3.11	Surface morphology of 1.27 mg cm ⁻² TiO ₂ /ENR ₅₀ /PVC loading at 1 000 x magnification.	126
Plate 3.12	Surface morphology of 1.27 mg cm ⁻² TiO ₂ /ENR ₅₀ /PVC loading at 50 000 x magnification.	126
Plate 3.13	Surface morphology of 2.22 mg cm ⁻² TiO ₂ /ENR ₅₀ /PVC loading at 1 000 x magnification.	127
Plate 3.14	Surface morphology of 2.22 mg cm ⁻² TiO ₂ /ENR ₅₀ /PVC loading at 50 000 x magnification.	127
Plate 3.15	Cross section area of TiO ₂ /AC/ENR ₅₀ /PVC at 0.32/0.63 (mg cm ⁻²) loading at 1 000 x magnification.	129
Plate 3.16	Cross section area of TiO ₂ /AC/ENR ₅₀ /PVC at 1.27/0.63 (mg	129

	cm ⁻²) loading at 1 000 x magnification.	
Plate 3.17	Cross section area of TiO ₂ /AC/ENR ₅₀ /PVC at 2.22/0.63 (mg cm ⁻²) loading at 1 000 x magnification.	130
Plate 3.18	Cross section area of TiO ₂ /AC/ENR ₅₀ /PVC at 0.32/0.63 (mg cm ⁻²) loading at 1 000 x magnification.	135
Plate 3.19	Cross section area of TiO ₂ /AC/ENR ₅₀ /PVC at 0.32/1.27 (mg cm ⁻²) loading at 1 000 x magnification.	136
Plate 3.20	Cross section area of TiO ₂ /AC/ENR ₅₀ /PVC at 0.32/2.54 (mg cm ⁻²) loading at 1 000 x magnification.	136
Plate 3.21	Surface morphology of TiO ₂ /ENR ₅₀ /PVC layer in TiO ₂ /AC/ENR ₅₀ /PVC bilayer before run at 1 000 x magnification.	180
Plate 3.22	Surface morphology of TiO ₂ /ENR ₅₀ /PVC layer in TiO ₂ /AC/ENR ₅₀ /PVC bilayer before run at 50 000 x magnification.	180
Plate 3.23	Surface morphology of TiO ₂ /ENR ₅₀ /PVC layer in TiO ₂ /AC/ENR ₅₀ /PVC bilayer after ten runs at 1 000 x magnification.	181
Plate 3.24	Surface morphology of TiO ₂ /ENR ₅₀ /PVC layer in TiO ₂ /AC/ENR ₅₀ /PVC bilayer after ten runs at 50 000 x magnification.	181
Plate 3.25	Surface morphology of AC/ENR ₅₀ /PVC layer in TiO ₂ /AC/ENR ₅₀ /PVC bilayer before run at 100 x magnification.	182
Plate 3.26	Surface morphology of AC/ENR ₅₀ /PVC layer in TiO ₂ /AC/ENR ₅₀ /PVC bilayer after run at 50 000 x magnification.	183
Plate 3.27	Surface morphology of AC/ENR ₅₀ /PVC layer in TiO ₂ /AC/ENR ₅₀ /PVC bilayer after ten runs at 100 x magnification.	183
Plate 3.28	Surface morphology of AC/ENR ₅₀ /PVC layer in TiO ₂ /AC/ENR ₅₀ /PVC bilayer after ten runs at 50 000 x magnification.	184

LIST OF ABBREVIATIONS

AC	Activated carbon
AC/ENR ₅₀ /PVC	Activated carbon/ epoxidized natural rubber/polyvinyl chloride single layer system
BET	Brunauer-Emmet-Teller
CHN	Carbon, Hydrogen, Nitrogen
COD	Chemical oxygen demand
e ⁻	Negatively charged electron
EDX	Energy dispersive X-ray
ENR ₅₀	Epoxidized natural rubber of 50 % mole epoxidation
FTIR	Fourier transform infra red
h ⁺	Positively charged hole
O ₃	Ozone
pH _{pzc}	pH at point of zero charge
PL	Photoluminescence
PVC	Poly (vinyl) chloride
SEM	Scanning electron micrograph
TGA	Thermogravimetric analysis
TiO ₂	Titanium dioxide
TiO ₂ /AC/ENR ₅₀ /PVC	Titanium dioxide/ activated carbon/epoxidized natural rubber/polyvinyl chloride bilayer system
TiO ₂ /ENR ₅₀ /PVC	Titanium dioxide/epoxidized natural rubber/polyvinyl chloride single layer system
UV	Ultraviolet
W	Watt

SISTEM DWILAPISAN TiO₂/KARBON TERAKTIF TERIMMOBIL UNTUK PENYINGKIRAN FENOL MELALUI PROSES FOTOPEMANGKINAN- PENJERAPAN

ABSTRAK

Titanium dioksida (TiO₂) dan karbon teraktif (AC) telah digabungkan dalam satu sistem pemegunan susunan dwilapisan di atas plat kaca untuk penyingkiran fenol. Sistem monolapisan AC/ENR₅₀/PVC dan dwilapisan TiO₂/AC/ENR₅₀/PVC terpegun telah berjaya dibangunkan melalui kaedah penyaduran celup mudah. Pelekat yang digunakan dalam larutan penyaduran celup mudah AC/ENR₅₀/PVC dan TiO₂/ENR₅₀/PVC ialah campuran ENR₅₀/PVC. Tujuan pemegunan ialah untuk menyingkirkan fenol daripada larutan akues secara fotopemangkinan dan dibandingkan dengan kaedah lama iaitu kaedah ampaian. Kajian kinetik dan isoterma penjerapan ke atas AC/ENR₅₀/PVC dan TiO₂/AC/ENR₅₀/PVC juga telah dijalankan yang mana kedua-dua sistem mengikut model kinetik aturan kedua Lagergren tetapi untuk kajian isoterma, sistem AC/ENR₅₀/PVC mengikut Langmuir manakala sistem TiO₂/AC/ENR₅₀/PVC mengikut isoterma Freundlich. Berat optimum AC/ENR₅₀/PVC adalah 2.54 mg cm⁻² manakala berat TiO₂/ENR₅₀/PVC di atas lapisan AC/ENR₅₀/PVC dalam sistem dwilapisan TiO₂/AC/ENR₅₀/PVC adalah 0.32 mg cm⁻². Didapati bahawa sistem dwilapisan TiO₂/AC/ENR₅₀/PVC berfungsi melalui gabungan dua proses secara serentak iaitu penjerapan fenol ke dalam lapisan AC/ENR₅₀/PVC dan fotopemangkinan fenol oleh lapisan TiO₂/ENR₅₀/PVC. Lapisan TiO₂/ENR₅₀/PVC mengikut pemalar kadar aturan pseudo pertama Langmuir Hinshelwood manakala lapisan AC/ENR₅₀/PVC menunjukkan kadar aturan pseudo kedua. Oleh yang demikian, TiO₂/AC/ENR₅₀/PVC mengikut pemalar kadar aturan kedua kerana proses penjerapan lebih baik daripada proses

fotopemamngkinan di dalam sistem dwilapisan. Kesan-kesan parameter seperti pH larutan, keamatan cahaya dan bekalan O₂ juga dikaji dan didapati optimum masing-masing pada pH larutan 6, 6 W m⁻² kebocoran UV dan 100 mL min⁻¹ kadar pengudaraan. Perbandingan di antara TiO₂/AC/ENR₅₀/PVC dan TiO₂/ENR₅₀/PVC adalah berdasarkan keefisienan penyingkiran fenol untuk semua parameter yang dikaji. Kadar mineralisasi fenol dikaji melalui ujian Keperluan Oksigen Kimia. Kebolegunaan dan ujian Keperluan Oksigen Kimia juga telah dijalankan di bawah iradiasi cahaya matahari untuk aplikasi asas. SEM-EDX, BET, FT-IR, CHN, PL dan TGA adalah merupakan beberapa pencirian fizikal digunakan untuk menerangkan fenomena sebelum dan selepas aplikasi.

IMMOBILIZED TiO₂/ACTIVATED CARBON BILAYER SYSTEM FOR THE REMOVAL OF PHENOL VIA PHOTOCATALYTIC-ADSORPTIVE PROCESSES

ABSTRACT

Titanium dioxide (TiO₂) and activated carbon (AC) had been combined in an immobilized bilayer arrangement on glass plates for the removal of phenol. The immobilized monolayer AC/ENR₅₀/PVC and bilayer TiO₂/AC/ENR₅₀/PVC systems have been successfully fabricated via a dip-coating method. The adhesives used in both activated carbon and TiO₂ dip-coating solutions were ENR₅₀/PVC blends. The purpose of the fabrication was to photocatalytically remove phenol from aqueous solution as opposed to the conventional suspension method. Adsorption kinetic and isotherm studies of TiO₂/AC/ENR₅₀/PVC and AC/ENR₅₀/PVC were also conducted whereby both systems followed second order kinetic model of Lagergren's but for isotherm study, the TiO₂/AC/ENR₅₀/PVC system obeyed Langmuir whereas the AC/ENR₅₀/PVC system obeyed Freundlich. The optimum AC/ENR₅₀/PVC loading was 2.5 mg cm⁻² while the optimum TiO₂/ENR₅₀/PVC loading on the AC/ENR₅₀/PVC layer was 0.32 mg cm⁻². It was found that the TiO₂/AC/ENR₅₀/PVC bilayer system operated simultaneously via the incorporation of the two processes i.e adsorption of phenol into the AC/ENR₅₀/PVC layer and photocatalytic degradation of phenol by the TiO₂/ENR₅₀/PVC layer. The single layer of TiO₂/ENR₅₀/PVC followed pseudo first order rate constant of Langmuir-Hinshelwood equation whereas the single layer of AC/ENR₅₀/PVC showed the pseudo second order rate constant. Therefore, TiO₂/AC/ENR₅₀/PVC followed the pseudo second order rate constant since the adsorption process was more favourable than the photocatalytic process in the bilayer system. The effects of some operational parameters such as pH of

the solution, light intensity and O₂ supply were also studied and were found to be optimized at pH 6, 6.0 Wm⁻² of UV leakage and 100 mL min⁻¹ of aeration rate, respectively. The comparison between TiO₂/AC/ENR₅₀/PVC and TiO₂/ENR₅₀/PVC was based on the removal efficiency for all the parameters studied. The mineralization of phenol was observed through COD test. The reusability and COD tests were also done under solar irradiation for practical applications. SEM-EDX, BET, FT-IR, CHN, PL and TGA are some physical characterizations used to describe the process phenomenon before and after applications.

CHAPTER 1: INTRODUCTION AND LITERATURE REVIEWS

1.1 Water Pollution: Law Enforcement, Treatment and Remediation Technology

About 70% of earth surface is surrounded by water. This abundance source of water is essential for the sustenance and continuation of all living things. The generation of electricity, crops plantation, and others are water-dependence in nature that carry economical values for a nation as well as the whole world. The increasing human population means increasing activities that somehow generate waste discharges that pollute the water sources. The discovery of new findings results in a growth of many kinds of industries such as pharmaceuticals, textiles, plastics, cosmetics and etc. The industrial wastes usually contained numerous types of chemical as well as biological species like algae, pathogens and viruses of fatal diseases that contribute towards acute toxicity in the contaminated water.

For decades, researchers and scientists have been continuously searching for the best method to treat the effluents and wastes before they are released to the mainstreams. The government and private sectors made an effort in funding researches in universities in order to gain the best method for wastewater remediation. Apart from that, many acts and enforcements had been established in order to protect the environment from an environmental disorder. As in Malaysia, the Environmental Quality Act 1974, Act 127 Section 29 [1] stated that,

(1) No person shall, unless licensed, discharge environmentally hazardous substances, pollutants or wastes into the Malaysian waters in contravention of the acceptable conditions specified under section 21.*[Am. Act 636:s.12]*.

(2) Any person who contravenes subsection (1) shall be guilty of an offence and shall be liable to a fine not exceeding five hundred thousand ringgit or to imprisonment for not exceeding five years or to both. *[Am. Act A953:s.15]*

The current technologies in wastewater remediation had pursued a great innovative development than the earlier pioneers of the technology. The flocculation, activated sludge, and carbon adsorption, are some examples of existing and conventional techniques that are now vastly considered as not that effective in terms of poor treatment of pollutant, cannot be re-used, costly, as well as generating secondary pollutants. A new concept of green technology reveals the need of decomposition and mineralization of pollutants into harmless compound as the final products such as CO₂, H₂O and NH₄⁺, NO₃⁻ and other mineral species. The ideal and green chemistry is said to be having the following characteristics as indicated in Table 1.1 [2-3]:

Table 1.1: Characteristics of ideal and green chemistry

Cost effective	Design for energy efficiency
Use of renewable feedstock	Prevention
Reduce derivatives	Mineralize toxic species
Catalysis	Atom economy
Design for degradation	Safer solvents and auxiliaries
Stable	Designing safer chemicals
Real-time analysis for pollution prevention	Safer chemistry for accident prevention

In general, there are three types of treatment to remove pollutants from the wastewater; physical, biological and chemical. Table 1.2 shows some of the applications of the three modes of water treatment technologies. However, the drawbacks that led to a decrement in the removal efficiency and reusability of each treatment technique tend to diminish the ‘dream’ of ideal and green wastewater

Table 1.2: Available technologies for use in the wastewater treatment

Treatment modes	Processes	Operation
Biological	Microbial degradation	Degradation using microbial xenobiotic metabolism [4]
	Adsorption by microbial biomass	Accumulation of organics/inorganics in microorganism [5]
	Bioremediation	Microorganisms to mitigate/eliminate hazardous pollutants [6]
	Enzymatic treatment	Phase transfer or partial polymerization of tyrosinase, laccase and horseradish peroxidase enzymes [7]
Physical	Nanofiltration	Membrane pretreatment using microfiltration and ultrafiltration [8]
	Reverse osmosis	Pressure-driven processes occur by solution-diffusion mechanism [9]
	Electrodialysis	Membrane-based separation process to separate ionic species using electrically charged membrane and electrical potential difference [10]
	Adsorption	Adsorption is a separating process in which the adsorbates are attracted to the interior and exterior surfaces of adsorbent [11]
Chemical	Coagulation/Flocculation	Use of coagulants and flocculants in solid-liquid separation processes [12]
	Electroflotation	Float pollutants by their adhesion onto tiny bubbles of H ₂ and O ₂ from electrolysis of aqueous. [13]
	Electronic coagulation	Generates metallic OH flocs in situ via electro-dissolution of a soluble anode [14]
	Oxidation (ozone)	Ozone (O ₃) acts as oxidant for organic pollutants to low molecular weight substances [15]
	Irradiation	Exposure of pollutants to the source of radiant energy [16]
	Advanced Oxidation Process (AOP)	Pollutant oxidation occurs via highly reactive intermediate, the hydroxyl radical(HO [•]) [17]

treatment technology. Biological treatment for example suffers from the sewage that are non-biodegradable, production of inert matter as well as toxic metabolites from the microbial metabolism of contaminants [18].

1.2 Phenol

The discovery of phenol (hydroxybenzene) at the end of eighteenth century made a history to scientists at that moment. Firstly isolated in crude form, pure phenol was then isolated in 1834 and the structure was proven in 1842. Classical uses of phenol included as wound dressing and antiseptic in surgery. Phenol exists as a white solid in pure form, possesses a sweet but irritating smell and can dissolve well in water and organic solvent despite of moving slower than water in the air. The products originated from phenol normally easy to catch fire and get burnt [19].

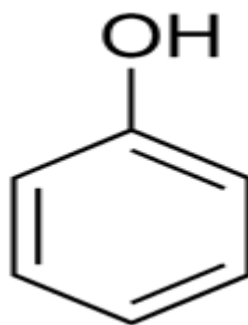


Figure 1.1: Molecular structure of phenol

For industrial scale, phenol was largely synthesized (<95%) from the extraction of coal tar formed by the transformation of high quantities of cumene present in plants that were used for the tar production. Apart from that, other

chemical reactions that produce phenol are alkylation of benzene with propene, chlorobenzene and sodium hydroxide as well as toluene-benzoic acid oxidation process. In nature, phenol is formed from various sources such as chemical reactions in condensed water vapour that forms clouds at atmosphere, biosynthesis by plants, decomposition of organic matter, tyrosine transformation in mammalian digestive tract and from amino acids contained in plants' hemicelluloses under the influence of sun rays [20].

At present, phenol is utilized to make plastics, nylon 6 and other man-made fibers as well as bisphenol A for the production of epoxy and other resins. Large amount of phenol is generated from oil refineries, coal gasification, petrochemical units, as well as leachates emerging from waste disposal produced by microbial hydrolysis and the photodegradation of organophosphorous pesticides [21]. In addition, the manufacturing industries and wasteland filling release many phenol-based chemicals into the atmosphere, groundwater, surface water bodies as well as soils and rocks [7]. With so many listed sources producing phenol, it is undeniable that our water sources are in harm of phenol contamination. It is also no doubt that phenol was one of the first compounds inscribed in The List of Priority Pollutants by the US Environmental Protection Agency (EPA) with the maximum amount of 1 mg L⁻¹ permitted in water bodies [22].

Phenol possesses carcinogenic, teratogenic and mutagenic properties as well as causes histopathological changes and acute toxicity for man's health. The toxicity of phenol stems from unspecified toxicity related with hydrophobicity of the individual compound, formation of free radicals and localization of the meta-para substituent. For example, phenolic compounds can mimic the oestradiol hormones that influence the development and maintenance of female characteristics while

bisphenol A may function as endocrine disrupting chemical. The active transformation of phenol after penetration of the cell membrane may form electrophilic metabolites that can bind and damage DNA or enzymes [20, 23].

The structure of phenol and its properties made it the parent of multi compounds that are produced in the industries such as chlorophenol, catechol, nitrophenol, bisphenols, aminophenols and methylphenols. Since phenol is a stable compound, the breakdown of its compound onto linear chain compound seems a big challenge. In addition, when phenol-containing water is chlorinated, the removal of toxic chlorinated phenolic compounds from the wastewater source to a safety level (0.1-1.0 mg L⁻¹) is not an easy task [23]. Moving on to the world of environmental green policy, it is an urge to find the ideal wastewater treatment that would solve the problem of removing this toxic and anthropogenic compound. Owing to this, advanced oxidation process (AOPs) can be a suitable candidate.

1.3 Environmental Photocatalysis

Advanced Oxidation Processes (AOPs) got its name from the chemical oxidation based process via hydroxyl radicals. A few methods that were based on AOPs are ozonation (O₃, O₃/UV, O₃/H₂O₂ and O₃/UV/H₂O₂), UV processes (UV and UV/H₂O₂), photocatalytic process (TiO₂/UV, semiconductor/UV) and Fenton process (H₂O₂/Fe²⁺, H₂O₂/Fe³⁺) [17]. Among those mentioned processes, photocatalysis is nearly closed to being the ideal and the most prominent treatment method in meeting clean energy demand and solving environmental pollution. A total number of 10,624 publications until the year 2010 (Source: ISI Web of Knowledge, 13/05/2011, search terms: “photocatalysis”) had been recorded which proved that there was a dramatic

rise of interest in photocatalysis. Its wide attractive applications are namely: water splitting of hydrogen generation, self-cleaning activity, air purification, degradation of pollutants in wastewater as well as carbon dioxide remediation [24].

In the environmental photocatalysis for wastewater treatment, molecules such as pesticides (herbicides, insecticides, fungicides, etc.) or dyes are totally destroyed and mineralized into CO_2 and innocuous inorganic anions (Cl^- , SO_4^{2-} , NO_3^-) [25]. Beside the selective mild oxidation of organic pollutants, many toxic inorganic ions can also be oxidized to their upper oxidation state which is harmless. For example, SO_3^{2-} is oxidized to SO_4^{2-} whereas CN^- to OCN^- and subsequently to NO_3^- and CO_3^{2-} . Heavy metal cations such as Pd^+ , Hg^+ , Ag^+ can be deposited as crystallites on TiO_2 surface after reduction by photoelectrons. Noble metal such as photographic Ag could be removed and separated from common metals baths [3]. In addition, this hydroxyl radicals-based reaction is the most viable method that can remove pollutants to a level as low as ppb (part per billion) [26].

Photocatalysis mediated semiconductor can operate under visible and UV region. In UV region, UV light with different wavelengths that range from UVC (200-290 nm), UVB (290-320 nm) and UVA (320-400 nm) can be used for the photocatalytic irradiation sources. For clinical issue, UVB can excite the DNA's molecules whereas UVA can generate reactive oxygen species in nucleic acids, proteins and lipids. UVC rays, on the other hand, have less clinical interest since they do not reach earth's surface. UV rays can cause skin damage such as erythema, immuno suppression, skin cancers and photo aging via the interaction between molecular components with epidermis and dermis [27]. However, in photocatalysis, ultraviolet (UV) irradiation source stands up among other sources due to the high energy band gap of some semiconductors. Since sunlight is an abundantly natural

energy source for UV irradiance, its energy can be conveniently exploited for the irradiation of semiconductor. In this case, the photocatalytic material must have high activity in regards to the process of interest with high efficiency of solar energy conversion. Semiconductor such as ZnO, ZnS, SnO₂ and TiO₂ are some examples of photocatalyst that have lower band gap energy and applicable for solar irradiation in photocatalysis for degradation of tons of organic effluents.

Instead of having good photoactivity, ZnO for example, has photochemical instability which normally yields Zn(OH)₂ and Zn²⁺ upon irradiation of the ZnO particles in aqueous media [28]. Similar problem arises with CdS photocatalyst which releases Cd²⁺ ions leading to heavy metal pollution in the treated water samples. In addition, both photocatalysts suffers from the photocorrosion from self oxidation. Meanwhile, metal sulphide and α -Fe₂O₃ semiconductors also face the same problem due to photoanodic corrosion of the former and photocathodic corrosion of the latter [29]. TiO₂ on the other hand is not only highly effective for producing oxidizing species (specifically \cdot OH radicals which possess significant oxidation potential) but also possess other advantages that include biological and chemical stability, photo stability, non-toxicity, low cost and availability [30]. Those criteria ensure that no problems may arise upon the TiO₂ photocatalytic degradation and mineralization processes of the organic pollutants especially due to the generation of secondary pollutants.

1.4 Titanium Dioxide as photocatalyst

Titanium dioxide (TiO₂) is the most prominent semiconductor among others since TiO₂ itself satisfies the ideal photocatalyst's criteria for being relatively stable,

non-toxic (final product of harmless compound, CO₂ and H₂O) and inexpensive [31]. The band gap energy of TiO₂ of 3.2 eV (anatase) and 3.0 eV (rutile), as well as high value of refractive index (n = 2.7) make TiO₂ as an effective UV absorber and a protector of substances from UV because of rapid attenuation offered via its light absorption and scattering properties. The interaction between UV radiation and the TiO₂ surface would generate oxidative free radicals that can degrade organic contaminants [32].

TiO₂ can exist in natural crystalline forms of anatase, rutile and brookite and also artificial form (TiO₂-B, TiO₂-H) [33]. The crystallographic forms of TiO₂ determined the photoactivity of the catalyst although the quantitative differences between the rutile and anatase forms are not that transparent. It was proven that the surface recombination of the photogenerated electrons and positive holes are higher in anatase phase than in rutile phase [14]. Anatase phase in the TiO₂ crystallographic form was also reported to have good photoactivity than rutile phase although they possess similar structure of octahedral chain (TiO₂⁻⁶). The reasons for this behavior could be related to the greater reflectivity for UV-visible light possesses by anatase phase though crystallite density and absorption ability of light in rutile phase is more dominant. Despite its low photoactivity, rutile form of TiO₂ has been reported to be an effective opacifier/UV protector for polymer in TiO₂ nanoparticles composites [32].

The main function of TiO₂ in the environmental photocatalysis is the photocatalytic oxidation of inorganic or organic water and air contaminants [34-35]. TiO₂ is widely used as the semiconductor that produces free radicals that can undergo reactions initiated by UV lights. The reaction is initialized when the photon energies are adsorbed by TiO₂ that results in the excitation of an electron (e⁻) from

the valence band to the conduction band of the TiO₂, and leaving behind an electron vacancy hole (h⁺) in the valence band. The photon has energy equal or greater than the band gap of the photocatalyst. The electron–hole pairs can either recombine or participate in chemical reactions on the surface of the photocatalyst. The ability of the pollutants molecules to be adsorbed on the photocatalyst surface will play a role on their photodegradation [35]. The mechanism of the TiO₂ reactions at the surface is given in Figure 1.2. The reactions associated with the mechanism of the charged induced reactions are provided by Equations 1.1 to 1.11.

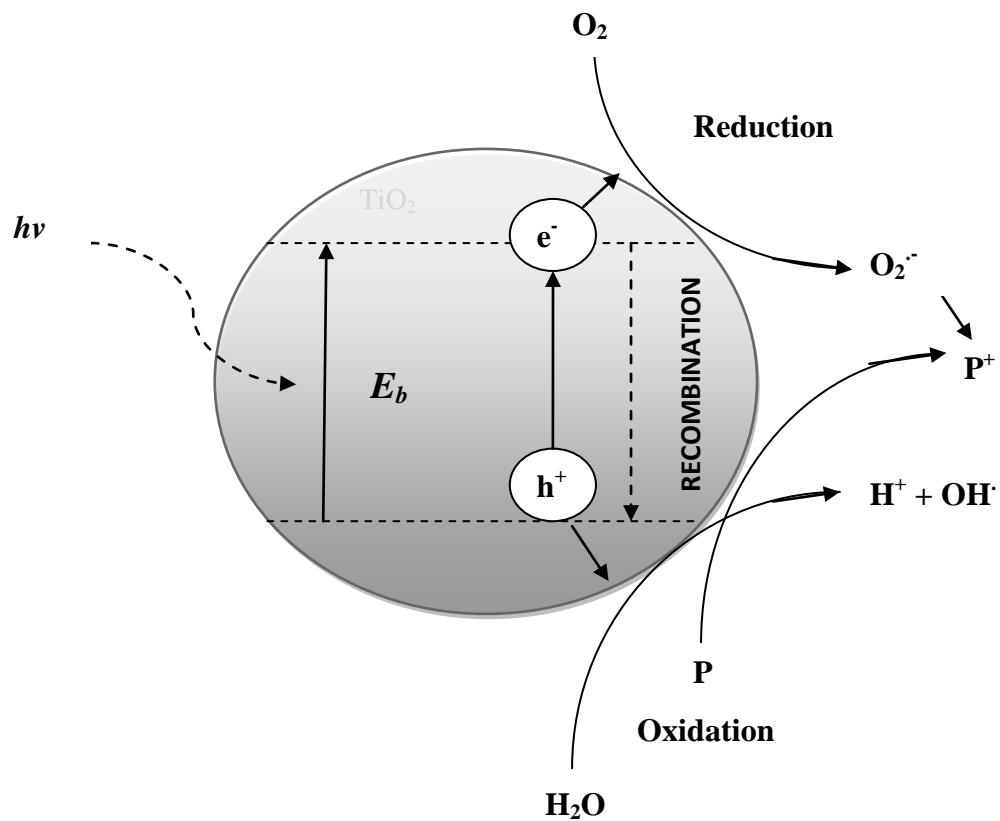
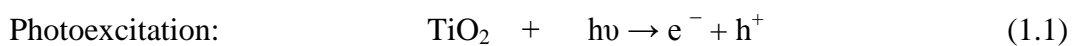
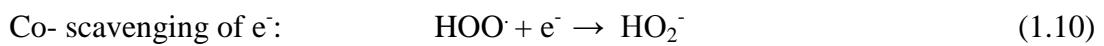
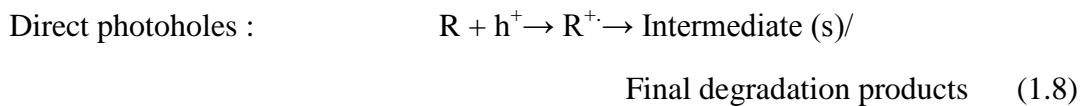
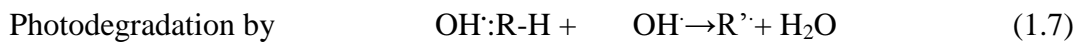
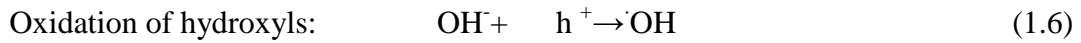
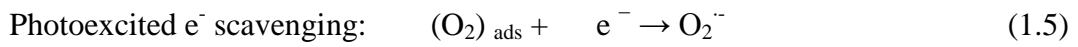
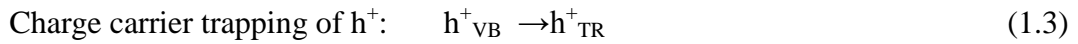


Figure 1.2: Schematic diagram of TiO₂ photocatalysis mechanism [36]





The highly reactive radicals that are formed on the surface of TiO₂ can react with the adsorbed organic pollutants resulting in the mineralization of the pollutants into harmless compounds.

1.5 Commercial TiO₂

The increasing interest on the multi-functional TiO₂ had provoked a demand in the TiO₂ production commercially where TiO₂ with commercial name such as Hombikat UV 100, PC 500 Millenium, Sigma, and Degussa P-25 (now known as Aeroxide® P-25) are currently available in the global market. Comparatively, the commercially available TiO₂ powder differed in terms of structure, particle size and surface area. Degussa P-25 had been reported to have high photoactivity due to the low recombination of electron and holes, whereas the high photoactivity in Hombikat

UV 100 TiO₂ powder is related to its fast interfacial electron transfer rate. Anyhow, the main factor that influences the physical properties is the specific production process of those catalysts that resulted in different surface concentration of active sites [37]. The same authors had investigated the influence of physical parameters of different types of TiO₂ samples on the adsorption kinetic studies of the oxalic acid. They concluded that the equilibrium behaviour of all samples was similar but differed in the measured degradation kinetic rates of the oxalic acid due to the morphological and porosity differences of the TiO₂ samples. Indeed, the geometry and chemistry of the TiO₂ samples also reflects the different level of adsorption and desorption rates of the adsorbates on the TiO₂ active surfaces. Table 1.3 below shows some available commercial TiO₂ and their respective physical properties.

Table 1.3: Commercial TiO₂ and their properties

Commercial TiO ₂ Properties	Degussa P-25	Hombikat UV100	PC500-Millennium	Sigma
Crystallographic phase	Anatase: rutile	Anatase	Anatase	Anatase
Ratio (%)	70:30, 80:20	100:0	> 99	>99
Specific area (m ² g ⁻¹)	50	300	>320	9-10
Ave particle size (nm)	35	20-30	5-10	< 25
Synthesis	Flame pyrolysis of TiCl ₄	Sulfate process, precipitation	N/A	N/A
References	[38]	[38]	[39]	[40]

In this research, TiO₂ Degussa P-25 was selected due to its versatility towards oxidation of organic contaminants and best known as the standard material in photocatalytic field [41]. About 4428 published articles were found under the

search word: Degussa P-25 via ScienceDirect browser whereas 1150 articles were found in ISI Web of knowledge database. The reported amount of articles as shown in Figure 1.3 evidently suggested the better reputation exhibited by Degussa P-25 than other commercially available photocatalysts. As listed in the previous Table 1.3, Degussa P-25 had two crystallographic phases; anatase and rutile that are produced from the flame pyrolysis synthetic process. During the process known as Aerosil process, titanium tetrachloride, $TiCl_4$ is subjected to hydrolysis process at elevated temperatures in a vapor phase within a continuous reactor which eventually produced the nanosized TiO_2 P-25 particles [41].

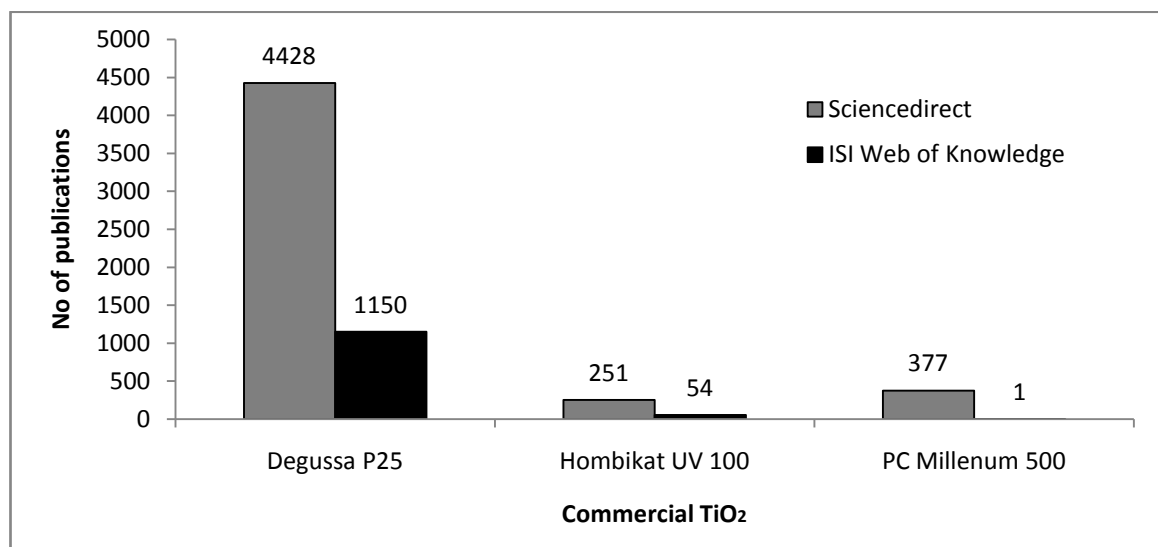


Figure 1.3: Number of publications on commercial TiO_2 .
Source: Sciencedirect.com (accessed on 12.10 am 23rd May 2011)

Ohno et al. [42] had carried out investigation on the synergism between rutile and anatase TiO_2 particles in the photocatalytic oxidation of naphthalene. Enhanced photoactivity was observed when both particles were simply mixed together. They deliberately proposed that there were electrons transfer occurring

from the rutile particles (produced under high temperature and large in size) to the anatase particles (produced under low temperature and small in size). For their case with naphthalene, they suggested that the molecules were mainly oxidized on rutile particles whereas oxygen was reduced on anatase particles.

The latest article published by Ohtani and his group [43], studied the comparison on activities of the original P-25, isolated anatase and rutile particles and reconstructed P-25. They concluded that all the phases (anatase, rutile and amorphous) in P-25 behave independently which were in opposite conclusion to the Ohno's group [42] proposal on anatase-rutile interaction that had been mentioned earlier. Nevertheless, TiO₂ consisting of anatase/rutile composition in both studies showed the enhanced performance of the photocatalytic oxidation of the pollutants. However, TiO₂ Degussa P-25 and its comparative performance as the photocatalyst was not the main focus in this study. The literature reviews were purposely done to highlight the history, argument and current information on TiO₂ Degussa P-25 as the standard photocatalyst in the photocatalytic oxidation reaction. TiO₂ is used throughout this thesis as to refer to TiO₂ Degussa P-25.

1.6 Photodegradation kinetic

In general, the photodegradation of organic pollutants by TiO₂ is observed to be well fitted by first order reaction. It follows the Langmuir–Hinshelwood model, where the reaction rate is proportional to the surface coverage, according to the following equation:

$$r = \frac{dC}{dt} = \frac{1}{K_c + K_C} \quad (1.12)$$

The above equation can be simplified to the pseudo first order kinetic equation at low concentration by integrating with respect to time, t .

$$\ln\left(\frac{C_0}{C}\right) = kKt = k_{app}t \quad (1.13)$$

where;

r : the rate of phenol degradation (min^{-1});

C_0 : the initial concentration of phenol (ppm);

C : the concentration of phenol at time t (ppm);

t : the irradiation time (min);

k_{app} : the reaction rate constant (min^{-1});

K : the adsorption coefficient of the phenol onto the photocatalyst particle (l/rag).

1.7 Adsorption

Adsorption is a separating process in which the adsorbates such as molecules, atoms and ions in the solvent (eg: water) are attracted to the interior and exterior surfaces of the solid namely adsorbent, on which adsorption occur through physical and chemical reactions. Generally, the adsorption of the adsorbate is influenced by pH, adsorbate concentration, size and type of adsorbents, time of interaction between the adsorbate and the adsorbent, the characteristics of the adsorbent surface and the present of the foreign substances that compete for the adsorption sites on the adsorbent. The adsorption of adsorbate onto the adsorbents can be explained by a comprehensive understanding of the nature of the interaction between the adsorbate with adsorbents for the most effective use of the adsorbent. A correlation of the

equilibrium data with the different relevant models of isotherm is essential to formulate a pragmatic program for design, operation, and optimization of the system.

The schematic diagram shown in Figure 1.4, explained the three components of adsorption process and their interactions. The main interaction force that controls the adsorption process is the affinity between the adsorbent and the adsorbate. However, the affinity between the adsorbate and the solvent (i.e. solubility) can also contribute a major role in the adsorption of adsorbate, for example; hydrophobic compounds have low solubility and tend to be ‘pushed’ to the adsorbent surface. Therefore, the compound is less adsorbed as opposed to the highly soluble ones.

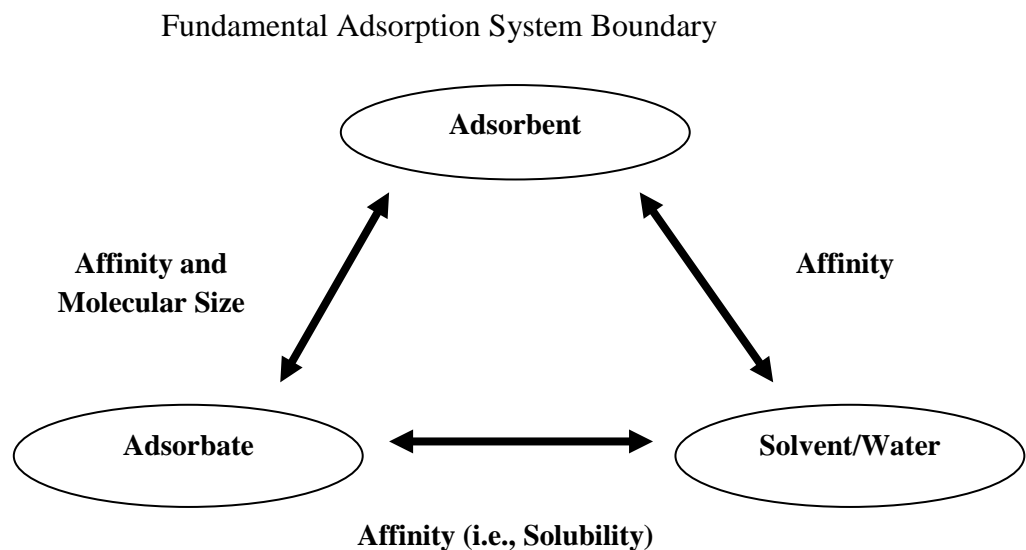


Figure 1.4: Schematic diagram of relationships between the three components of the adsorption system [44]

1.8 Activated Carbon (AC)

Adsorption by the activated carbon has been widely applied in the wastewater treatment of industrial effluents for the removal of dye, odor, organic and inorganic pollutants as well as for air pollutants. Up until now, the activated carbon is continuously being produced from various types of carbonaceous material.

Inexpensive materials such as wood, coconut shells, fruit stones, coals, lignites and petroleum coke have high carbon content and low inorganic content which are suitable for activated carbon precursors. The selection of the raw materials depends on the possibility of generating activated carbon with high adsorption capacity, density and hardness, have low inorganic matter as well as its easy availability and low in cost [45]. Some general forms of AC are shown in Table 1.4.

Table 1.4: Type of ACs and their properties [45]

Type of AC	PAC (Powdered Activated Carbon)	GAC (Granular Activated Carbon)	ACF (Activated Carbon Fiber)
Diameter	Less than 0.15 mm	0.5 to 2.5 mm	10 to 40 μm
Applications	Various locations in a treatment system	Fixed-bed adsorbers such as granular media filters or post filters	Fibers or as thin cloths in the treatment of gas or liquid streams at elevated flow rates
Advantages	Can interact directly with the contaminants in water	(i) Effective for adsorption of gases and vapors (ii) Has great mechanical strength	(i) Excellent mechanical properties (ii) Low thermal expansion coefficient, (iii) High thermal and electrical conductivities (iv) Low hydrodynamic resistance

According to Radovic et al. [46], the adsorption capacity of an activated carbon depends on:

- a) *The nature of the adsorbent* (e.g. functional groups present, surface area and pore size distribution, ash content).

- b) *The nature of the adsorbate* (e.g. functional groups present, polarity, hydrophobicity, molecular weight and size, solubility and pK, or pK, for weak electrolytes).
- c) *Solution conditions* (e.g. pH, temperature and adsorbate concentration, presence of competitive solutes, polarity of solvent).
- d) *Activation process* (chemical and physical activation using precursor such as ZnCl₂, H₂SO₄, H₃PO₄ and etc).

Generally, the porous structure of ACs consists of small amounts of chemically bonded heteroatoms (mainly oxygen and hydrogen) and in addition of mineral matter, usually ash content up to 20% of initial mass. The heterogeneity of ACs surfaces are normally associated with the geometrical and chemical sources in which the former is affiliated with the differences in size and shape of pores, cracks, pits and some steps while the latter is a contribution of different functional groups at the edges of the turbo static crystallites as well as other surface impurities. The impurity that was adsorbed on activated carbon was mainly dispersed by Van der Waals's forces. The pores in AC are classified based on their origin, size and state. Table 1.5 defines this classification.

Table 1.5: Classification of AC pores [47]

Class of pores	Type of pores	Shape of pores
<u>Origin-based</u>	Intraparticle pores	Intrinsic intraparticle pores Extrinsic intraparticle pores
	Interparticle pores	Rigid interparticle pores Flexible interparticle pores
<u>Size-based</u>	Micropores < 2 nm	
	Mesopores 2-50 nm	Ultramicropores < 0.7 nm
	Macropores > 50nm	Supermicropores 0.7-2 nm

<u>State-based</u>	Open pores Closed pores	(Latent pores)
--------------------	----------------------------	----------------

Due to the chemical nature of activated carbon, its affinity towards polar molecules such as water and molecules of nitrogen or oxygen at room temperature is very low. However, for non-polar organic molecules, its affinity is high. For activated carbon to play its role efficiently, the internal surface area must be large enough, usually ($500-1500 \text{ m}^2 \text{ g}^{-1}$), to be accessible to the adsorbing molecule. In general, knowledge in surface area of the carbon materials is essential since the physiochemical properties of carbons are strongly influenced by the chemical species on the surface of AC. The oxygen-containing functional groups of carbon determine the acidic and basic characteristics of the adsorbent with the former usually are formed via oxidative treatment while the latter are formed from the decomposition of the acidic groups (i.e., carboxylic acid, lactone and phenol group) heated at high temperatures. Other carbon surface chemical reactions may also involve nitrogen-, hydrogen- sulphur-, phosphorus-, halogens and boron-containing functionalities [48].

There are many methods of producing activated carbon whereby thousands of them have been patented and registered worldwide. All of these production methods can be classified into two distinguished groups: thermal (physical) activation and chemical activation. The thermal activation generally consists of two steps which are carbonization of the raw material at medium or high temperatures to produce a char and activation step where the remaining char is partially oxidized in direct fired furnaces. If both steps are simultaneously carried out, the process is called direct activation. The chemical activation on the other hand, is carried out in a single carbonization stage where the raw material is impregnated with chemical agent (mostly used H_3PO_4 , ZnCl_2 and alkaline hydroxides). The product is washed to

remove any excess chemical agent after carbonization. Figure 1.5 shows the basic flow sheet of activation processes of activated carbon.

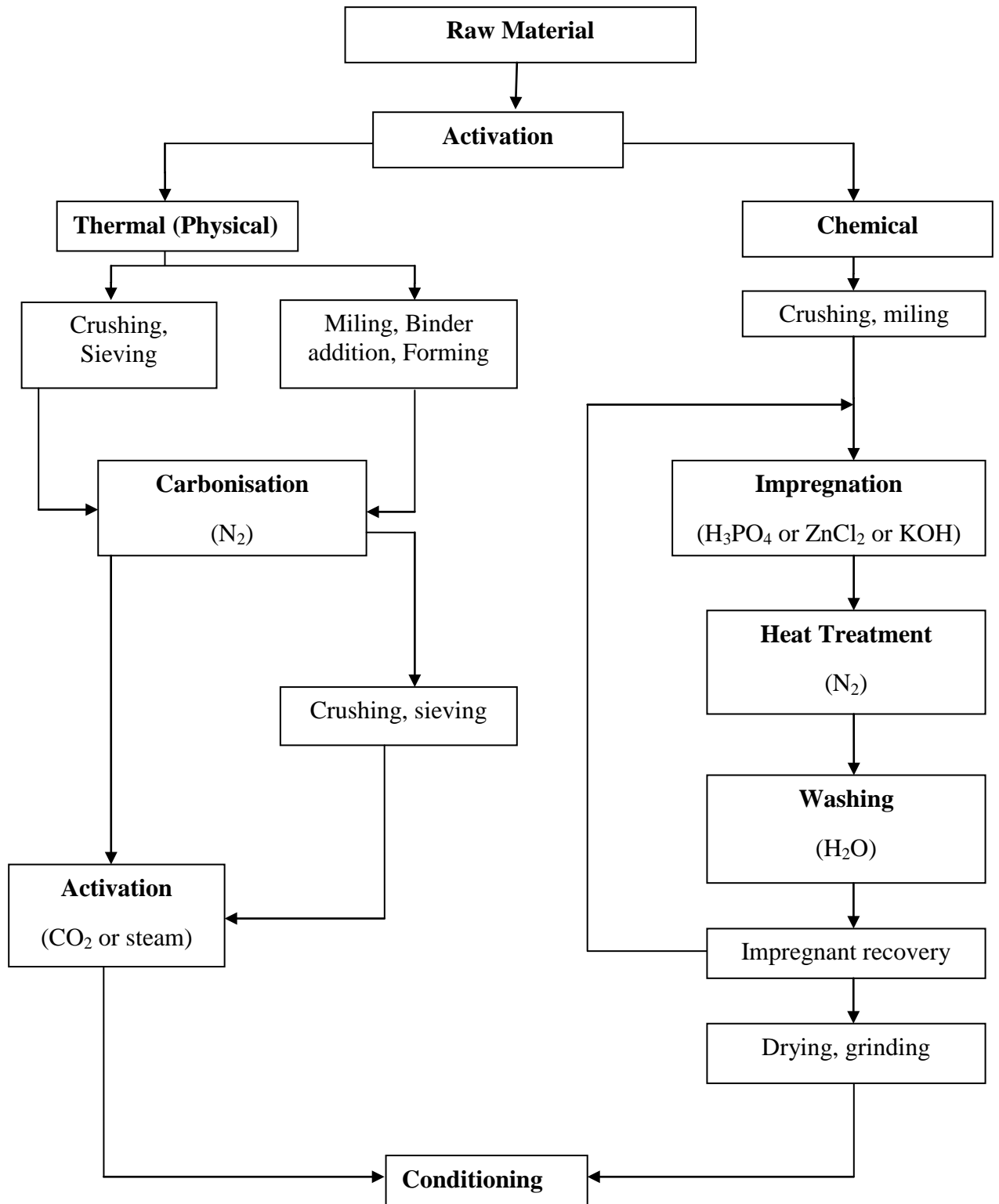


Figure 1.5: Basic flow sheet for activation of activated carbon [49]

1.9 Adsorption kinetic

The investigation on the kinetic that governs an adsorption system as well as the rate determining step is crucial for designing a large scale adsorption system. In order to elucidate the mechanism of adsorption and potential rate controlling steps such as mass transport and chemical reaction processes, a few kinetic models have been proposed to fit the experimental data. Three common kinetic models that generally used in adsorption studies are pseudo first order, pseudo second order and intraparticle diffusion.

1.9.1 Pseudo first order [50]

Lagergren's pseudo first order equation is represented as follows;

$$\frac{dq_t}{dt} = k_1 (q_e - q_t) \quad (1.14)$$

After integration and applying boundary conditions at $t=0$ to $t= t$ and $q_t=0$ to $q_t=q_t$, the equation becomes;

$$\log (q_e - q_t) = \log q_e - \left(\frac{k_1}{2.303} \right) t \quad (1.15)$$

where q_e and q_t are the adsorption capacity at equilibrium (mg g^{-1}) and at time (t), respectively and k_1 is the rate constant of pseudo-first order sorption (min^{-1}). A straight line plot of $\log (q_e - q_t)$ against time (t) will give k_1 and q_e from the slope and intercept, respectively.

1.9.2 Pseudo second order

For second order adsorption mechanism where chemisorption is the rate controlling step, the equation is expressed as;

$$\frac{dq_t}{dt} = k_2 (q_e - q_t)^2 \quad (1.16)$$

For which after integration, the equation becomes,

$$\frac{t}{qt} = \frac{1}{k^2 q_e^2} + \left(\frac{1}{q_e}\right)t \quad (1.17)$$

Where k_2 is the rate constant of pseudo-second order ($\text{g mg}^{-1} \text{min}^{-1}$). A straight line plot of $\log t/q_t$ against time (t) will give k_2 and q_e from the slope and intercept, respectively.

1.9.3 Intraparticle diffusion

Initial adsorption generally occurs on the surface of the adsorbent whereby there is a possibility of the adsorbate to diffuse into the interior pores of the adsorbent [51]. In 1962, Weber and Morris proposed an intraparticle diffusion model which is based on an empirically found function relationship (in adsorption process), where uptake varies almost proportionally with $t^{1/2}$ rather than the contact time t . The equation is shown in equation 1.18.

$$q_t = k_d t^{1/2} + C \quad (1.18)$$

where k_d ($\text{mg g}^{-1} \text{h}^{1/2}$) is the intraparticle diffusion rate constant and is calculated by plotting q_t versus $t^{1/2}$.

1.9.4 Elovich model

This model is mainly applicable to chemisorption kinetics in the systems in which the adsorbing surface is heterogeneous [52]. The Elovich model is presented as

$$\frac{dq_t}{dt} = \alpha e^{-\beta q_t} \quad (1.19)$$

Integrating this equation for the boundary conditions, gives

$$q_t = \frac{1}{\beta} \ln(\alpha\beta) + \frac{1}{\beta} \ln t \quad (1.20)$$

where, α = the initial adsorption rate (mg/ g min) and β = surface coverage and activation energy for chemisorptions (g/mg). The graph is calculated by plotting q_t versus $\ln t$.

1.10 Combination of photocatalysis and adsorption processes as a single system

To date, most of the studies had successfully followed Langmuir Hinshelwood kinetic model which described the photocatalytic degradation of the respective pollutants. However, in the novel $\text{TiO}_2/\text{AC}/\text{ENR}_{50}/\text{PVC}$ bilayer system, the $\ln C_0/C_e$ may not give good agreement with the pseudo first order linearised equation (linear regression values of $r^2 < 0.9$) due to the influence of the adsorption process on the overall removal rate of the pollutant. Since most of the adsorption processes follow pseudo second order kinetics, so, for this study, the involving a bilayer system of $\text{TiO}_2/\text{AC}/\text{ENR}_{50}/\text{PVC}$, evaluation of the kinetics should be evaluated also on the pseudo second order kinetic rate equation.

The second order kinetic was based on the simultaneous process i.e, photocatalysis by TiO₂ layer and adsorption by AC layer, on the removal of phenol that occurred in the bilayer system. Under the experimental conditions, there were a few assumptions which have to be considered in following the second order kinetic models such as;

1. The adsorption of phenol by activated carbon should be the dominant process as compared to the TiO₂ photocatalysis.
2. The occurrence of the two processes, photocatalysis and adsorption occur simultaneously.

Under the second order reaction, the equation becomes,

$$\frac{1}{C} = \frac{1}{C_0} + k_{app}t \quad (1.21)$$

Equation 1.21 can be rearranged to give equation 1.22,

$$\frac{1}{C_0} - \frac{1}{C} = k_{app}t \quad (1.22)$$

where, a graph of 1/ C versus t is plotted to obtain the slope of the graph which represents the pseudo second order apparent kinetic rate constant where the unit will be in M min⁻¹.

1.11 The equilibrium adsorption isotherm models

The adsorption of adsorbate onto the adsorbents needs a comprehensive understanding of the nature of the interaction between the adsorbate with adsorbents

for the most effective use of the adsorbent. Therefore, the equilibrium adsorption isotherm theories were developed in order to understand the mechanisms of the system and the fundamental interaction between the solutes (adsorbates) and the adsorbent in an adsorption system [53]. The adsorption process of adsorbate into the adsorbent can be explained by using several models of the equilibrium isotherms which are listed in Table 1.5. Among them are the two most popular models namely Langmuir and Freundlich models. The two models are usually used in the adsorption of solid-liquid system. Initially, the adsorption capacity which was the amount of adsorption at equilibrium is computed as follows:

$$\text{Adsorption capacity } (q_e) = \left(\frac{C_o - C_e}{W} \right) V \quad (1.23)$$

C_o = initial adsorbate concentration

C_e = final or equilibrium concentration of adsorbate (mg/L)

W = weight of the adsorbent (g)

V = volume of the adsorbate solution (mL)

However, despite of the two famous isotherm models, there are some other models which were introduced later in order to understand the adsorption mechanism that failed to be explained by the former two models. They were Temkin, Brunauer-Emmett- Teller (BET), Dubinin-Radushkevich (D-R) and Elovich isotherms. The equations fitted for each model are given in Table 1.6. The details of the isotherm models are also provided in Table 1.6.